Studies of the Cat's Medial Interlaminar Nucleus: A Subdivision of the Dorsal Lateral Geniculate Nucleus

KENNETH E. KRATZ,[1] SARAH V. WEBB AND S. MURRAY SHERMAN
Department of Physiology, University of Virginia School of Medicine, Charlottesville, Virginia 22901

ABSTRACT The medial interlaminar nucleus (MIN) of the cat lies medial to the laminated region of the dorsal lateral geniculate (lamLGN). This latter region includes the A and C laminae. As does lamLGN, MIN receives direct retinal input and projects to various visual cortical areas. We examined the MIN of 15 normal adult cats with electrophysiological and anatomical techniques.

Autoradiographs processed from cats that had one eye injected with tritiated fucose and proline indicate that MIN is composed of at least two laminae, one for each eye. The area which receives input from the ipsilateral eye is a small central region surrounded dorsally, medially, and ventrally by a larger crescent shaped region that receives input from the contralateral eye. This pattern was also evident from electrophysiological recording experiments.

Extracellular recordings from 102 single-units in MIN indicate that these cells have properties essentially identical to lamLGN Y-cells. That is, they had short latencies to orthodromic stimulation of the optic chiasm and antidromic stimulation of the visual cortices, responded in a phasic manner to the presentation of a standing contrast within the receptive field center, responded to rapidly moving visual stimuli, and showed non-linear spatial summation properties typical of lamLGN Y-cells. We discovered two differences between MIN cells and lamLGN Y-cells. First the mean receptive field center size of MIN cells is considerably larger than that of lamLGN Y-cells, and second, MIN cells do not have the non-dominant eye inhibitory receptive fields found for many lamLGN Y-cells.

Cell size measurements indicate that while the mean cell size in MIN is approximately 30% greater than in the A laminae of lamLGN, the distribution of MIN cell sizes extends over the full range of cell sizes in the A laminae. Since the A laminae are comprised mostly of X- and Y-cells, this suggests that, although Y-cells on average are larger than X-cells, considerable overlap exists in their size distribution. No differences between the ipsilateral and contralateral terminal zones were found on any measure.

Since MIN cells share most or all the fundamental features of lamLGN Y-cells, we suggest that these cell groups should be considered subpopulations of a more general group of geniculate Y-cells. Accordingly, we refer to these two subpopulations as lamLGN Y-cells and MIN Y-cells.

The medial interlaminar nucleus (MIN) is a subdivision of the dorsal lateral geniculate nucleus of a number of carnivores, including the cat (Sanderson, '74). In the cat, MIN is located just medial to the laminated region of the lateral geniculate nucleus (lamLGN). Included in lamLGN are the A and C laminae. As does lamLGN, MIN receives direct retinal input (Hayhow, '58; Laties and Sprague, '66; Guillery, '70) and projects to the visual cortex. The areas of cortex to which these subdivisions project, however, are slightly different.

[1] Present address: Department of Anatomy, Louisiana State University School of Medicine, New Orleans, Louisiana 70112.

Whereas lamLGN projects predominantly to cortical areas 17, 18, and 19, MIN projects predominantly to cortical areas 18, 19 and the lateral suprasylvian visual areas, with at most a sparse projection to area 17 (Rosenquist et al., '74; Maciewicz, '74, '75; Gilbert and Kelly, '75; LeVay and Ferster, '77; Holländer and Vanegas, '77).

The part of the cat's retino-geniculo-cortical pathway which passes through lamLGN has been fairly extensively studied. Many investigators have provided evidence that this pathway is composed of at least three parallel and functionally distinct systems (Enroth-Cugell and Robson, '66; Cleland et al., '71; Hoffmann and Stone, '71; Hoffmann et al., '72; Stone and Dreher, '73; Wilson and Stone, '75). W-, X-, and Y-cells in retina project respectively to geniculate W-, X-, and Y-cells which, in turn, form three parallel, largely independent relays to cortex (Enroth-Cugell and Robson, '66; Cleland et al., '71; Hoffmann et al., '72; Stone and Dreher, '73; Wilson and Stone, '75). In lamLGN, X- and Y-cells can be located in all laminae, whereas W-cells are essentially confined to the C laminae (Wilson and Stone, '75). The significance of this parallel processing in terms of cortical neurons, however, is not clear (Hubel and Wiesel, '65; Stone and Dreher, '73; and others).

Geniculate W-, X-, and Y-cells in lamLGN have been distinguished by numerous receptive field properties and by response latencies both to orthodromic activation from the optic chiasm and also to antidromic activation from the visual cortex (Cleland et al., '71; Hoffmann et al., '72; Hoffmann and Stone, '71; Stone and Dreher, '73; Shapley and Hochstein, '75; Kratz et al., '78a). W-cells are distinguished by their slow axonal conduction velocities as well as a variety of receptive field characteristics. Compared to X-cells in lamLGN, Y-cells generally: (1) have shorter optic chiasm (orthodromic) and visual cortical (antidromic) response latencies, (2) sum visual stimuli across their receptive fields in a less linear fashion, (3) respond more briskly to rapidly moving visual stimuli, (4) have larger receptive field centers, and (5) give more phasic responses to standing contrast in the receptive field center.

Various short reports have recently indicated that, in constrast to lamLGN, MIN has only cells with Y-type characteristics. Palmer et al. ('75) have reported that all cells in MIN can be classified as Y-cells on the bases of optic chiasm latency, effective stimulus velocities, receptive field size, and spatial summation properties. Dreher and Sefton ('75) classified all MIN cells as Y-cells except for a small group of cells at the lateral border of the nucleus. This abstract however offers no details of neuronal classification. In addition, Mason ('75) found that the vast majority of MIN cells give brisk transient responses to a standing contrast in the receptive field center. The present study confirms and extends previous reports on the properties of single cells in MIN.

METHODS

The MIN of 15 normal adult cats were studied. Of these, nine cats were used for electrophysiological experiments, three cats for neuroanatomy, and three cats for both.

Electrophysiology

Preparation and recording

Standard, single-unit extracellular recording techniques were used to study the electrophysiological properties of cells in MIN of 12 cats. Cats were anesthetized with halothane in N_2O/O_2 (50%/50%) for surgery and with N_2O/O_2 (70%/30%) during the recording session. The animals were paralyzed with a continuous infusion of Flaxedil (19 mg/hour) in Ringer's with 5% dextrose. They were artificially ventilated, and their end-tidal CO_2 was maintained at 4.0%. Atropine and Neosynephrine were used to dilate the pupils and retract the nictitating membranes, and the corneas were protected with zero-power contact lenses. Spectacle lenses, if needed, were chosen by retinoscopy to make the retinae conjugate with a white tangent screen 114 cm in front of the nodal points of the eyes. The optic discs were plotted onto the tangent screen using the technique of Fernald and Chase ('71).

Varnished tungsten microelectrodes (15-30 megohms at 500 Hz) were used to record single-unit extracellular potentials. The recording electrodes were inserted from above at a 30° angle to the vertical in the coronal plane so that the electrodes moved ventromedially (e.g., see fig. 2). This allowed the electrode to sample cells first in laminae A and A1, and from Sanderson's maps (Sanderson, '71) we were consequently better able to locate the relatively small MIN. Bipolar stimulating electrodes were placed stereotaxically in the optic chiasm. In some of the preparations,

electrodes were also inserted 1-2 mm into cortical areas 17 and 18 for antidromic activation of MIN cells. Electrical stimulation consisted of 50-100 μsec square-wave pulses of 0.25-3.0 mamps. Latencies of the response to stimulation of the optic chiasm and visual cortex were measured from the beginning of the stimulus artifact to the foot of the action potential (cf., Hoffmann et al., '72).

Plotting of receptive fields

All receptive fields in MIN were concentric in makeup, similar to those observed in lamLGN. Receptive field centers were plotted using small spots of light produced by a hand-held projector. The boundaries of the center were determined by moving the flashing light spot toward the center region from above and below and from either side of the center until a response was elicited from the center. The boundaries of the spots closest to the center of the receptive field were noted (cf., Hoffmann et al., '72). When these positions were marked, the perimeter of the field center was drawn as a circle or ellipse passing through the four marks.

Visual stimuli

Receptive field properties were studied using hand-held targets or stimuli produced by a computer-controlled optical system. Stimuli included light spots, black disks, and light bars. In addition, we used a constrast reversal stimulus, consisting of a 9° by 9° bipartite field in which illumination of the two sides was sinusoidally counterphased (see Kratz et al., '78a, for details). Light stimuli were approximately one log unit above a background illumination of 0.5-1.5 cd/m^2, and black targets were 0.27 cd/m^2 on a background illumination of 6.8 cd/m^2.

Histology

Histological verification

During the recording sessions, small electrolytic lesions were made to facilitate electrode track reconstructions. One or more lesions were made in at least one penetration on each side of the brain. At the end of the recording sessions, the cats were anesthetized with barbiturate and perfused with saline followed by 10% formol-saline. The brains were stereotaxically blocked, removed, and embedded in egg-yolk. Frozen sections were cut coronally at 40 μm and stained with cresyl violet. Electrode tracks were reconstructed with the aid of a drawing tube attached to a microscope. All units included in the present study were shown to be in MIN by track reconstructions.

Cell size measurement

The cross-sectional areas of cells in MIN and in lamLGN were measured in six cats. Three of the cats had been used for recording. The perfusion and tissue processing was the same as described in the preceding paragraph. Two of the cats were given injections of tritiated proline and fucose (500 μCi each) into the vitreous of one eye ten days before they were sacrificed, and these brain sections were processed by autoradiographic techniques (Cowan et al., '72) prior to staining. This enabled visualization of the regions of ipsilateral and contralateral termination of retinal afferents in MIN. Cell outlines were drawn at 1,000 × using the drawing tube microscope attachment, and cross-sectional areas were measured with a planimeter. Only cells with visible nucleoli were drawn, and previously described procedures (Sherman and Wilson, '75) were employed to avoid sampling biases.

RESULTS

Extracellular potentials were recorded from 102 single cells encountered along 42 penetrations through MIN in 12 cats. The electrophysiological properties of each cell were examined using a battery of tests. These properties were compared with similar properties among cells that were encountered by the electrode in lamLGN prior to its entering MIN (METHODS). Cells in lamLGN were classified as X- and Y-cells based on previously described criteria (see below; Hoffmann et al., '72; Kratz et al., '78a). Furthermore, the cell sizes of these neuronal groups were compared.

Lamination of MIN

Although no lamination is evident in Nissl-stained sections for MIN, experimental techniques indicate that MIN has "hidden" lamination (Guillery, '70). At least two laminae exist, one for each eye, and this was immediately clear from our autoradiographs. Figure 1 shows bright- and dark-field views of both lateral geniculate nuclei from a section treated for autoradiography and counter-stained with cresyl violet. Ten days before sacrifice, the cat's right eye was injected with tritiated proline and fucose. Thus the labelled zones of

the left lateral geniculate indicate the contralateral retinal projection, and labelled zones of the right lateral geniculate indicate the ipsilateral retinal projection. The regions centered on MIN and outlined in figures 1d,e are shown in higher magnification with brightfield illumination (figs. 1a,f), with darkfield illumination (figs. 1b,g), and with a brightfield/darkfield double exposure technique (figs. 1c,h). The heavily labelled area of the left MIN shows the contralateral retinal projection zone of the right eye (figs. 1b,c). The somewhat oval shaped central region, which remains unlabelled, shows the ipsilateral retinal projection zone of the left eye. As expected, the right MIN has the complementary pattern of labelling. The small labelled region (figs. 1g,h) receives input from the ipsilateral right eye and corresponds to the unlabelled region of the left MIN. The larger unlabelled region of the right MIN receives input from the contralateral left eye and corresponds to the labelled region of the left MIN. Therefore, the pattern of labelling indicates the hidden lamination: a central portion receiving ipsilateral retinal afferents surrounded dorsally, medially, and ventrally by a region of contralateral termination. The lateral border of MIN abuts lamLGN.

Electrophysiological properties

The locations of ipsilateral and contralateral units along our electrode tracks were consistent with the previously described pattern of retinal termination. Reconstructions of four penetrations through MIN are illustrated in figure 2. Figures 2A,B illustrate penetrations which passed through the middle part of MIN. During these penetrations, we recorded first from units driven by the ipsilateral eye and then from cells driven by the contralateral eye. When penetrations passed through more ventral or dorsal parts of MIN (figs. 2C,D), we encountered only units driven by the contralateral eye.

The visual field positions of the receptive fields of the units on each penetration are shown to the right of the reconstruction. As the electrode moved from the lateral to the medial border of MIN, the receptive fields progressed from the central to peripheral visual field. Further, when the electrode was moved rostrally in MIN, the receptive fields moved lower in the visual field. Although we have not yet constructed a complete map of the visual field representation in MIN, our preliminary findings are generally consistent with those of Sanderson ('71) and Kinston et al. ('69), in spite of the fact that these reports seemed unaware of the hidden lamination in MIN.

As the electrode passed ventromedially through lamLGN, consecutive receptive fields of encountered neurons moved progressively towards the vertical meridian. As the electrode passed out of lamLGN into MIN, the fields moved rapidly away from the vertical meridian. We used this field reversal as an indication that the electrode had passed into MIN. The exact location of the penetrations were later verified histologically. Often a reversal in the relative locations of successive receptive fields could not be detected until a fairly large shift away from the vertical meridian had occurred. Because of this, and to ensure that our sample was located in MIN, we collected data from few fields near the *area centralis*.

Of the 102 MIN cells studied, 101 had consistent and similar electrophysiological properties described in detail below. The one anomalous unit gave inconsistent responses and was not driven by optic chiasm stimulation. This unit may have been a rare interneuron (Lin et al., '77) and is not considered further. Therefore, the description below is limited to the aforementioned 101 MIN cells.

Fig. 1 Photomicrographs of coronal sections through the lateral geniculate nucleus of a cat. An injection of tritiated proline and fucose was made into the vitreous of its right eye ten days before sacrifice, and autoradiography was performed on the brain sections. The scale in a represents 500 μm for a-c; the scale in d represents 500 μm for d and e and the scale in f represents 500 μm for f-g.

a Brightfield view of the medial portion of the left lateral geniculate nucleus. The area is outlined by the dashed rectangle in d.

b Darkfield view of same region as a. The labelled zones are bright against a dark background and indicate terminal zones of axons from the right retina.

c Brightfield/darkfield double exposure of the same region as a. Shown are the A and C laminae as well as the "hidden" lamination in the medial interlaminar nucleus (MIN).

d Brightfield view of left lateral geniculate nucleus, showing the smaller zone (dashed rectangle) that is illustrated in a-c. MIN, the optic tract (OT) plus the A and C laminae are labelled.

e Brightfield view of right lateral geniculate nucleus as in d; the dashed rectangle outlines the area represented in f-h.

f-h Series of brightfield, darkfield and brightfield/darkfield double exposure photomicrographs as in a-c. Notice that the labelling pattern is complementary to that seen in a-c, and that the "hidden" lamination is also seen in MIN.

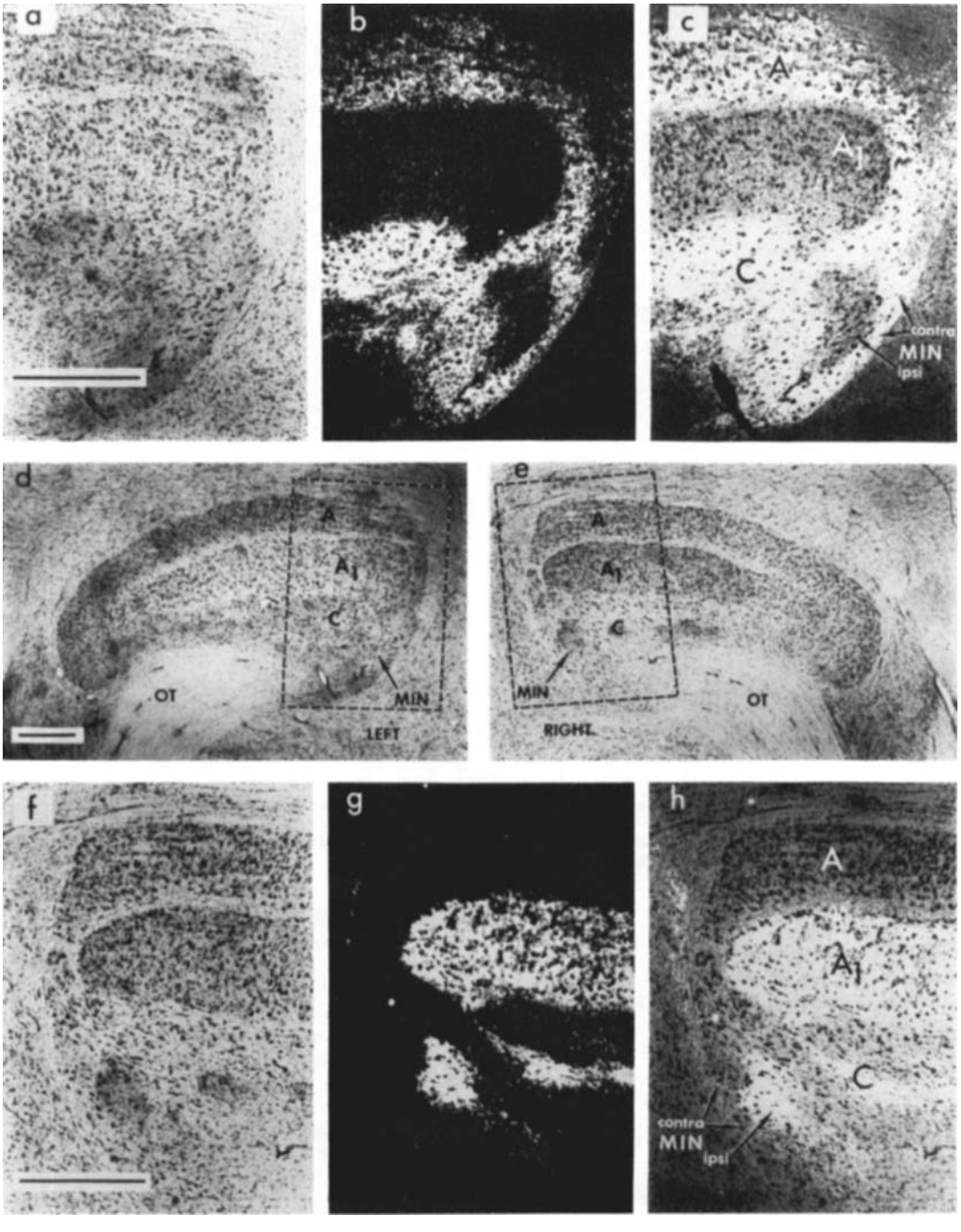
a
b
c
A
A1
C
contra
MIN
ipsi
d
A
A1
C
OT
MIN
LEFT
e
A
A1
C
MIN
OT
RIGHT
f
g
h
A
A1
C
contra
MIN
ipsi

Figure 1

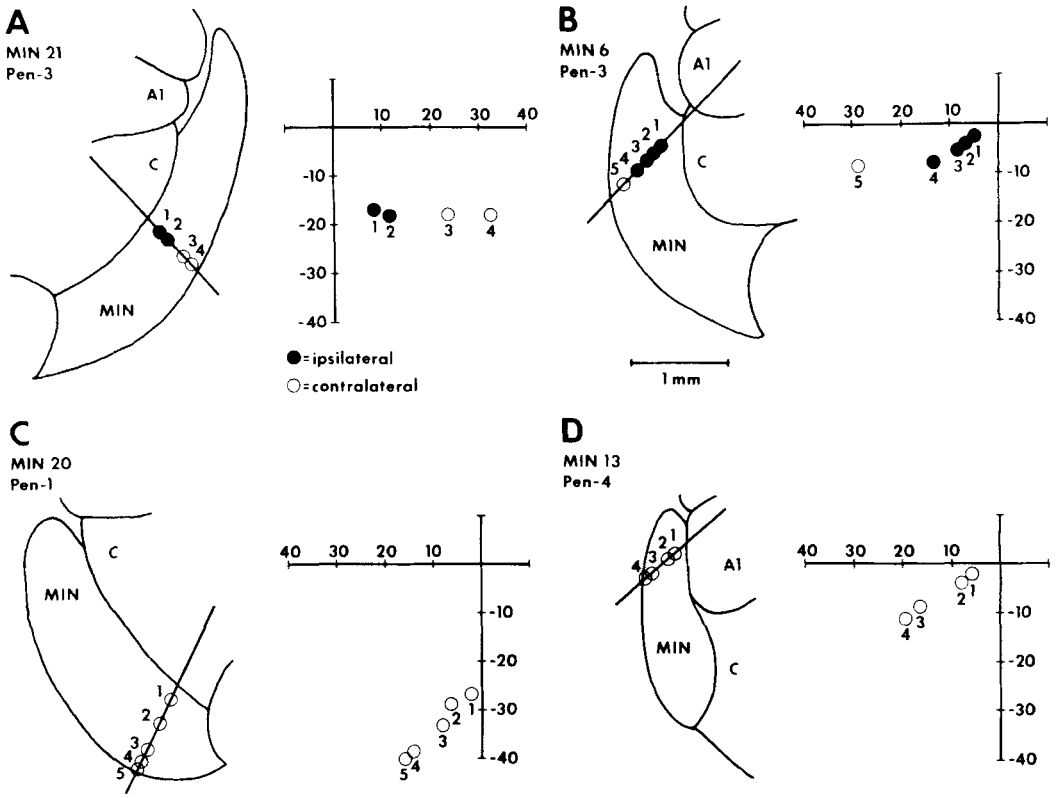

Fig. 2 Reconstructions of four electrode penetrations through MIN. On the left for each of the four is shown the electrode track (a straight line with circles). Each circle represents a single MIN cell. Cells driven by the contralateral eye are shown as open circles, and cells driven by the ipsilateral eye, as filled circles. To the right of each reconstruction is a quadrant of the visual field, with numbers along the axes indicating elevation (vertical axis) and azimuth (horizontal axis) in degrees. Circles show the locations of the receptive fields of corresponding numbered units on the electrode track reconstruction.

A, B Ocular dominance regions corresponding to hidden lamination for penetrations through center of MIN.

C, D Penetrations through ventral (C) and dorsal (D) portion of MIN. Here, only units driven by the contralateral eye were encountered.

Classification

Based on response latencies to chiasm and cortical electrical stimulation, spatial summation properties of the receptive field, responses to fast target movements, and responses to appropriate standing contrast, each of the 101 MIN cells had properties nearly identical to those of Y-cells in lamLGN.

Latencies to optic chiasm and visual cortex stimulation

Figure 3 depicts the frequency histograms of latencies to optic chiasm stimulation for MIN cells (fig. 3A) compared to X- and Y-cells encountered in laminae A and A1 (fig. 3B). The MIN cell latencies essentially match those of lamLGN Y-cells and have little overlap with those of X-cells. However, the mean latency for MIN cells is slightly shorter than that for lamLGN Y-cells (1.2 vs. 1.3 msec; $p < 0.02$ on a t-test). These latency differences may be due to different lengths of afferent axons and may not represent a significant difference in afferent conduction velocities.

Out of 23 MIN cells tested, 20 cells were antidromically driven by stimulation of area 17 and/or 18. From our data, we cannot ascertain whether a given cell was driven from one or both areas. The high ratio of antidromically activated cells is consistent with the high estimated ratio of relay cells in MIN (Lin et al.,

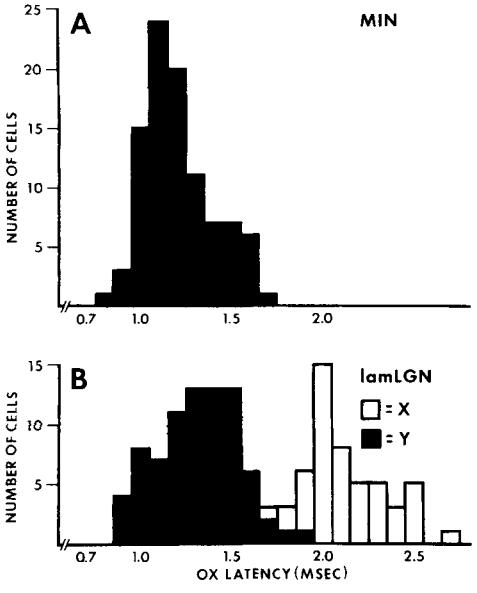

Fig. 3 Frequency histograms of response latencies to electrical stimulation of the optic chiasm (OX).

A Distribution of latencies of 95 MIN cells. The mean and standard deviation was 1.2 and 0.2 msec.

B Distribution of latencies of 79 A laminae Y-cells and 50 A laminae X-cells. The respective mean and standard deviation for each was 1.3 and 0.2 msec and 2.1 and 0.2 msec.

'77). In fact, because some MIN cells may project exclusively to areas beyond 17 and 18 (Rosenquist et al., '74; Maciewicz, '74, '75; Gilbert and Kelly, '75) and thus beyond the range of our stimulating electrodes, there is no reason to assume that the three cells not activated by cortical stimulation were not also relay cells. The latencies to cortical stimulation ranged from 0.4-1.2 msec, with a mean of 0.7 msec and standard deviation of 0.15. These values are essentially identical to those reported by Hoffmann et al. ('72) for antidromic latencies of Y-cells in lamLGN. However, we found no significant correlation between orthodromic (optic chiasm) and antidromic (visual cortical) latencies for MIN cells, whereas Hoffmann et al. ('72) reported such correlations for both X- and Y-cells in lamLGN. It should be emphasized that we measured response latency and not conduction velocity. Conduction velocity measurements conceivably could yield significant correlations for chiasm and cortical stimulation.

Spatial summation properties

Spatial summation properties of 76 MIN cells were tested with a contrast reversal stimulus (METHODS). The center of the bipartite stimulus was placed at various positions

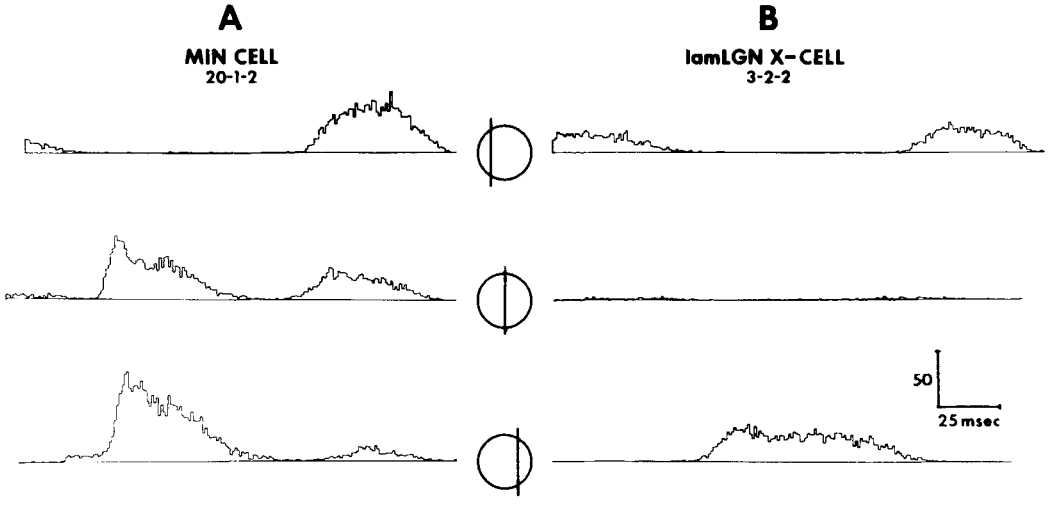

Fig. 4 Post-stimulus time histograms to the contrast reversal stimulus (see text) for a MIN cell and a lamLGN X-cell. Each of the three histograms shown for each cell illustrates the responses when the center of the bipartite stimulus was placed at one of three different locations in the cell's receptive field center. The circles represent the field center, and the line drawn through each circle indicates the position of the stimulus center for the adjacent histogram. The scales indicates 50 spikes/sec and 25 msec.

A Responses of MIN cell. Note the clear response at all stimulus positions.

B Responses of X-cell. Note the absence of response at the null (middle) stimulus position.

in the cell's receptive field in an attempt to locate a null position (i.e., a stimulus position which evoked little or no response from the cell). The presence of a null position indicates linear spatial summation typical of X-cells, while the absence of a null position indicates non-linear spatial summation typical of Y-cells (Enroth-Cugell and Robson, '66; Kratz et al., '78a). All MIN cells tested showed non-linear spatial summation properties. Figure 4 compares the responses of a cell in MIN and a lamLGN X-cell to this contrast reversal stimulus. The MIN cell (fig. 4A), like Y-cells in lamLGN, responded regardless of the position in the receptive field of the center of the bipartite stimulus. In contrast, the X-cell had a null position (middle histogram in fig. 4B).

Response to rapidly moving stimuli

Two tests were used to study the responses of MIN cells to rapidly moving stimuli. First, all cells were tested with a target which was much larger than the receptive field center of the cell and which was of appropriate contrast to excite the cell through its receptive field surround (i.e., a black disk for ON center cells and a light spot for OFF center cells). The target was moved by hand through the receptive field at 200-300°/sec. All MIN cells gave vigorous excitatory responses to this stimulus. This test has been used as one of the criteria for distinguishing between X- and Y-cells in lamLGN. Y-cells give excitatory responses to such a stimulus, whereas X-cells do not (Cleland et al., '71; Hoffmann et al., '72). Secondly, some cells were tested with a stimulus of appropriate contrast to excite the cell through its center. This stimulus was moved through the receptive field at various speeds ranging from 2-400°/sec. Figure 5A is a series of post-stimulus time histograms of the responses of an ON center MIN cell to a light bar moved through the receptive field at four different velocities. The cell shown in this figure, and all MIN cells we tested, continued to respond at stimulus speeds of 300-400°/sec. Y-cells in lamLGN also respond over this range of stimulus velocities, whereas geniculate X-cells generally do not respond at stimulus speeds greater than 100°/sec (Cleland and Levick, '74) (fig. 5B).

Response to standing contrast

We examined each MIN cell for the response to standing contrast in the receptive field center. Targets were slightly smaller than and confined within the receptive field center.

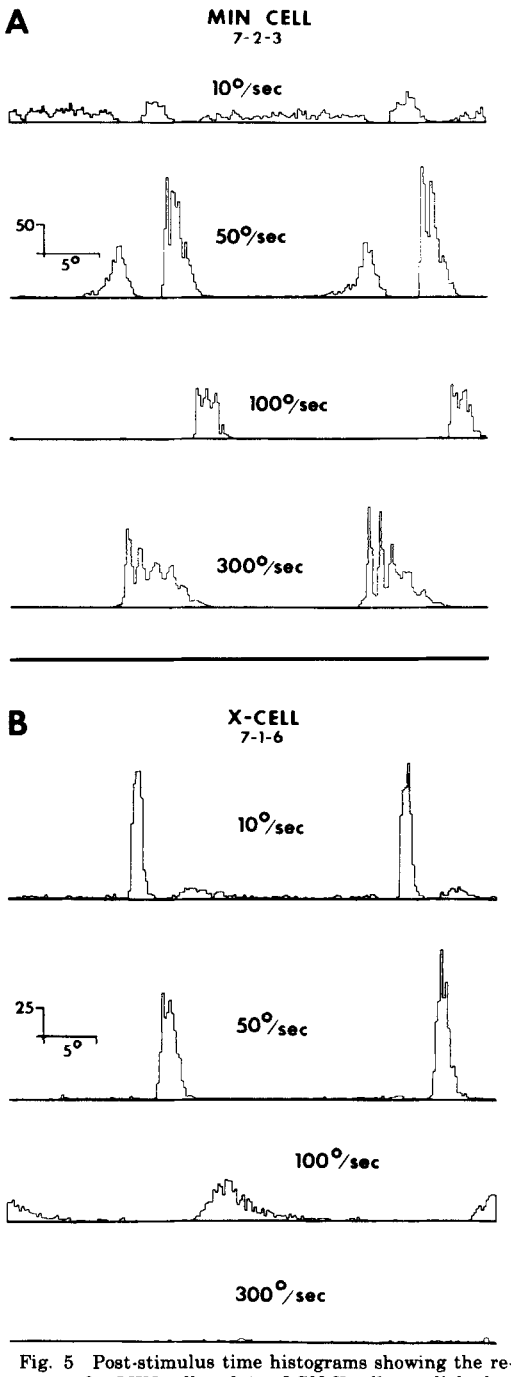

Fig. 5 Post-stimulus time histograms showing the responses of a MIN cell and lamLGN X-cell to a light bar moved through the receptive field at four velocities. The scales indicate 50 or 25 spikes/sec and 5°.

A Responses of MIN cell. The cell responds well at the highest stimulus speed (300°/sec) shown.

B Responses of X-cell. The cell responds relatively poorly at 100°/sec and not at all at 300°/sec.

Light spots were used for ON center cells, and black disks, for OFF center cells. The target was introduced into the center and the duration of the cell's response was timed. Units responding for less than five seconds were considered phasic. We found that all MIN cells showed phasic properties. Figure 6A shows a post-stimulus time histogram of the response of an ON center MIN cell to a light spot placed in the receptive field center for 20 seconds. At stimulus onset, the cell gave a burst of spikes, followed by a return to the spontaneous firing rate within two seconds. This type of response is typical of Y-cells in the A and C laminae, whereas geniculate X-cells generally exhibit tonic responses (Cleland et al., '71). Figure 6B illustrates the tonic response of a geniculate X-cell, which continued to respond slightly above its spontaneous level throughout the 20-second period that the stimulus remained in the center.

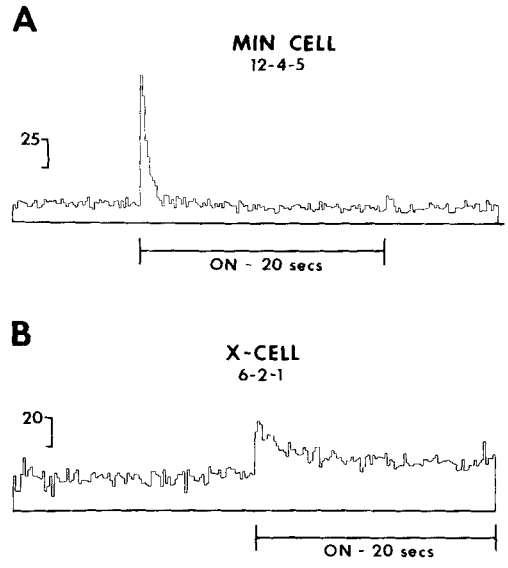

Fig. 6 Post-stimulus time histograms showing the responses of a MIN cell and lamLGN X-cell to a light spot placed in the receptive field center. Both cells were ON center. The spot was the size of the receptive field center and was on for 20 seconds and off for 20 seconds. Vertical scales indicate spikes per second.

A Responses of MIN cell to ten stimulus trials. The response is phasic and the firing rate returned to the baseline level within two seconds of the stimulus onset.

B Responses of X-cell to five stimulus trials. The response, while fairly weak, was sustained above the baseline level throughout the 20 second stimulus duration.

Binocular inhibition

All MIN cells in our sample could be excited through stimulation of only one (dominant) eye, and this is also typical of lamLGN cells. Most of these latter cells have, in addition to the excitatory field for the dominant eye, a purely inhibitory field for the non-dominant eye (Sanderson et al., '71). We also confirmed this for X- and Y-cells in laminae A and A1.

We examined 11 MIN cells for inhibitory fields related to the non-dominant eye. The field for the dominant eye was plotted and the corresponding area for the non-dominant eye was estimated from the relative positions of the optic discs (cf. Sanderson et al., '71; Bishop et al., '62). The dominant eye was then occluded, and a computer-controlled optical system moved a large bar of light repeatedly back and forth through this area. A post-stimulus time histogram relating stimulus position to neuronal firing rate was generated. An inhibitory field was seen as a drop in this firing rate below spontaneous levels.

Figure 7A shows the responses of a Y-cell from lamina A and three MIN cells to a bar stimulus moved across the receptive field of the dominant eye. The responses of these cells to the movement of the stimulus through the corresponding area of the non-dominant eye are illustrated in figure 7B. The Y-cell from lamina A showed a marked decrease in activity when the stimulus crossed this area for the non-dominant eye. In contrast, the activity of the MIN cells did not change when the stimulus moved through this area for the non-dominant eye. None of the 11 MIN cells examined showed evidence of inhibitory fields for the non-dominant eye, whereas three of four Y-cells in laminae A and A1 showed clear inhibitory fields for the non-dominant eye ($p < 0.01$ on a Fisher exact probability test). It is difficult to assess the significance of this difference between MIN cells and Y-cells of the A laminae, since the role played by these non-dominant eye inhibitory fields is unclear.

Center size as a function of eccentricity

We measured the diameter of the receptive field center of each MIN cell and determined the eccentricity of the receptive field with respect to the *area centralis*. The location of the *area centralis* was inferred from the position of the optic disc (Bishop et al., '62). In order to analyze center size as a function of eccentricity, we divided the cells into four eccentricity groups: 0-3°, 3-10°, 10-20°, 20-45°.

The mean receptive field center diameter for each group of MIN cells is plotted in figure

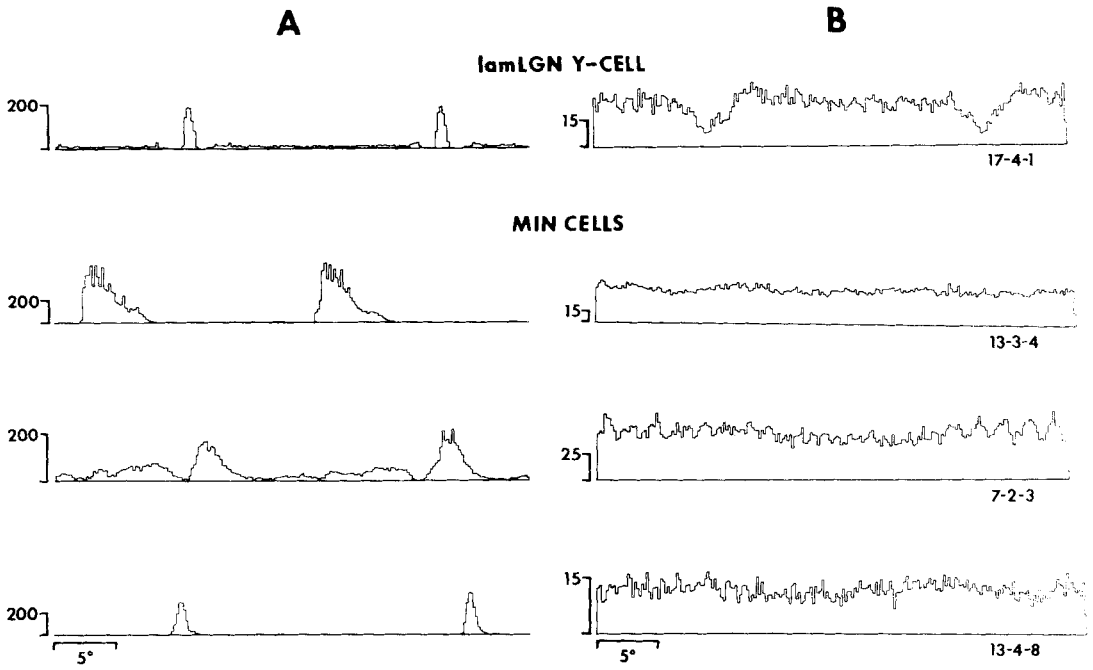

Fig. 7 Binocular inhibition tests for a lamina A Y-cell (top histograms) and three MIN cells (lower 3 histograms). The vertical scales indicate spikes per second.

A Excitatory responses evoked by movement of a bar stimulus through the receptive field of the dominant eye.

B Activity of the cells when the dominant eye was covered and the stimulus was moved through the corresponding region of the non-dominant eye's visual field. Compare the activity decreases evident in the histogram of the lamina A Y-cell with the flat histograms for the MIN cells.

8A. This figure also contains analogous values for lamLGN X- and Y-cells as reported by Hoffmann et al. ('72). These latter values are based on the same four eccentricity groups as the MIN data plus a fifth group (greater than 45°). MIN cell field size for the fifth group is not shown since we could find only two cells with fields in that eccentricity range.

In lamLGN, Hoffmann et al. ('72) found that the mean receptive field center size of Y-cells is greater than that of X-cells at every eccentricity, and that the field centers of both cell types increase in size with eccentricity in a fairly parallel fashion (fig. 8A). Our data indicate that the mean center size of MIN cells, compared to Y-cells and the A and C laminae, is greater at every eccentricity and shows a much larger increment in size with eccentricity.

Frequency histograms of receptive field center diameters of MIN cells and lamLGN Y-cells are shown in figure 8B for the four eccentricity groups. MIN cells in the 0-3° group have center sizes within the range of lamLGN Y-cell center sizes. In the other three eccentricity groups, while considerable overlap exists, the range of MIN field sizes extends at the upper end to as much as three times the diameter of the largest fields of lamLGN Y-cells.

Cell sizes

Cell sizes were measured in four matched zones of the lateral geniculate nucleus of six cats; MIN, lamina A1, the binocular segment of lamina A, and the monocular segment of lamina A. The boundaries of each sample area were well away from the borders of the A laminae or MIN. Thirty to sixty cells were measured in each zone. For measurements in MIN, we first used autoradiographic preparations in two of the cats (METHODS) to compare sizes of cells receiving ipsilateral retinal input with those receiving contralateral afferents. Since no significant difference was found between these two cell groups, subsequent measure-

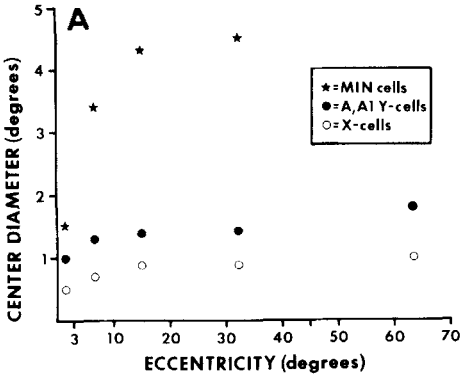

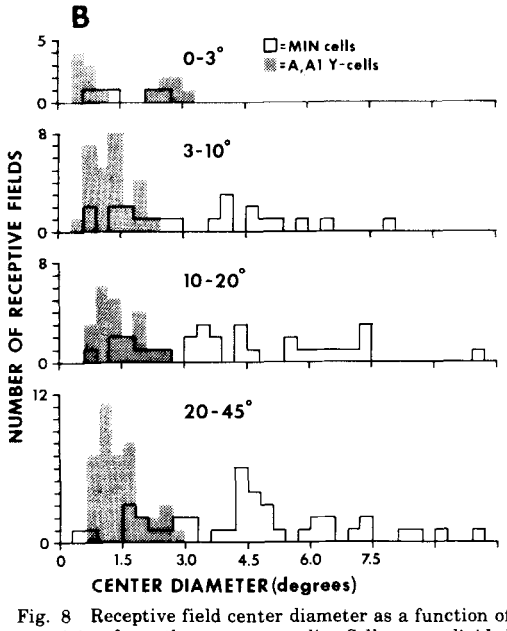

Fig. 8 Receptive field center diameter as a function of eccentricity from the *area centralis*. Cells were divided into five eccentricity groups: 0-3°, 3-10°, 10-20°, 20-45°, and > 45°.

A Mean center size for MIN cells (stars), lamLGN Y-cells (filled circles), and lamLGN X-cells (open circles).

B Frequency histograms of center diameters of MIN cells (open bars) and lamLGN Y-cells (shaded bars) in four eccentricity groups. Values for lamLGN X- and Y-cells are from Hoffman et al. ('72).

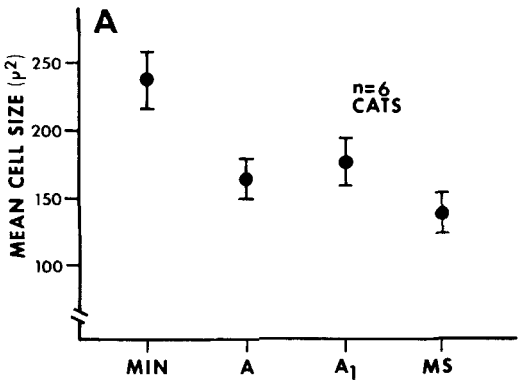

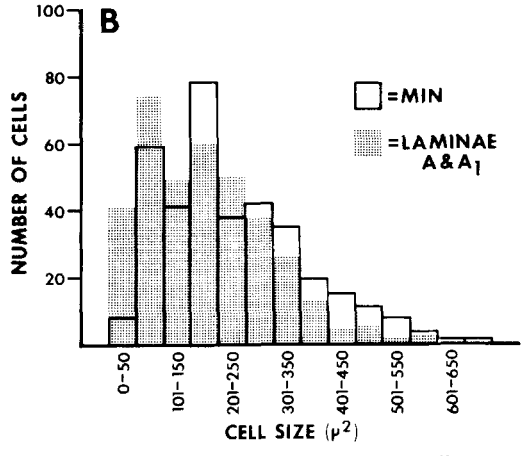

Fig. 9 Measurements of lateral geniculate cell sizes.

A Mean cell sizes in MIN, the binocular segment of lamina A, lamina A1, and the monocular segment of lamina A (MS). Thirty to sixty cells were measured from each of these sample areas. For each cat and each sample area, a mean was calculated and considered a single measurement. For each sampling area is shown the mean ± one standard error for these six single measurements.

B Frequency histograms of cross-sectional areas of cells in MIN (open bars) and in the A laminae (shaded bars).

ments were made from normal Nissl-stained material, and these samples were taken from the dorso-medial aspect of MIN.

The means of neuronal cross-sectional areas for MIN, the binocular portion of lamina A, the binocular portion of lamina A1, and the monocular segment of lamina A (MS) are plotted in figure 9A. The mean cell size in MIN is greater than in any of the other three geniculate regions, and the MIN cells are significantly larger than cells of lamina A which rank next ($p < 0.02$ on a t-test). Figure 9B compares a frequency histogram of cell sizes in MIN with a similar histogram for the A laminae. This illustrates that, even though larger on average, MIN cell sizes extend over the full range of cell sizes in the A laminae. Since few interneurons are found in these

areas, this implies that the smallest relay cells in MIN and in the A laminae are of roughly equal size (Lin et al., '77).

DISCUSSION

Classification and terminology

By all of the criteria for cell classification employed in this study (latency of response to optic chiasm stimulation, spatial summation properties, responses to rapidly moving stimuli, and responses to appropriate standing contrast), the 101 MIN cells were indistinguishable from lamLGN Y-cells. These results confirm and extend earlier reports (Palmer et al., '75; Dreher and Sefton, '75; Mason, '75). However differences can be noted between these groups. MIN has a dense projection to cortical areas 18, 19 and lateral suprasylvian visual areas, and at most a sparse projection to area 17, whereas lamLGN Y-cells, at least in the A laminae, project only to areas 17 and 18 (Rosenquist et al., '74; Maciewicz, '74, '75; Gilbert and Kelly, '75; Holländer and Vanegas, '77; LeVay and Ferster, '77); MIN cells do not display non-dominant eye inhibition as do many lamLGN Y-cells; and the distribution of MIN field sizes extends to values considerably larger than those of lamLGN Y-cells. Undoubtedly, other subtle differences exist. This raises the question as to whether MIN cells should be considered functionally distinct and fundamentally different from lamLGN Y-cells, or whether these should be considered as different subpopulations of geniculate Y-cells. We have decided, tentatively, upon the latter course and shall refer to these as "MIN Y-cells," "lamLGN Y-cells," etc. This terminology is based on the evidence suggesting that the Y-cell properties shared by these cells are considerably more fundamental than their differences. It must be recognized that this is largely an arbitrary assessment (see Rowe and Stone, '77, for a detailed consideration of this problem). Further support for the consideration of MIN cells as Y-cells is offered in the following paper (Kratz et al., '78b), since MIN cells and Y-cells in the A and C laminae suffer nearly identical deficits as a consequence of early eyelid suture, whereas X-cells are relatively unaffected.

The above interpretation does not suggest that there is merely redundancy in information processing by the Y-pathways. Differences listed above, especially differences in cortical projection areas and sizes of receptive fields indicate that the information transmitted by these two Y-pathways (MIN and lamLGN) may well subserve different functions for the animal's visual behavior.

It should be noted that previous investigators have reported a small population of X-cells (Dreher and Sefton, '75) or cells with sustained response to standing contrast (Mason, '75) at the lateral edge of MIN. Likewise, LeVay and Ferster ('77) found a group of small cells containing cytoplasmic laminar bodies, which they suggest are X-cells, at the lateral border of MIN. Unfortunately, we have not to our knowledge recorded from these cells. Since they lie at the lateral edge of MIN where the vertical meridian of the visual field is represented, we probably would not have been certain from their receptive field locations that they were in MIN, and thus they may have been ignored. Consequently, we cannot address the question of receptive field properties for these neurons.

Receptive field sizes

Not only do MIN Y-cells have larger fields than those of lamLGN, but the change with eccentricity is much greater for the former than for the latter. Hoffmann et al. ('72) reported that, for lamLGN, Y-cell fields increased in size slightly with increasing eccentricity from the *area centralis*, but this increase was matched in parallel fashion by X-cell fields. This at first seems different from analogous data for tree shrews (Sherman et al., '76), and owl monkeys (Sherman, Wilson, Kaas, and Webb, unpublished). For these animals, the increase in field size with eccentricity was considerably greater for Y-cells than for X-cells. If MIN and lamLGN Y-cells in the cat are now considered parts of a single Y-cell population, it is evident that data from cat will more closely correspond to those from tree shrew and owl monkey in this regard. That is, in the cat, fields of geniculate Y-cells (including MIN cells) increase with eccentricity at a rate much greater than do fields of X-cells.

Cell sizes

The cross-sectional area of MIN cells is slightly larger on average than that of cells in laminae A and A1. This suggests, in turn, that the MIN cells tend to be larger in volume than those in the A laminae. This conclusion, however, requires a qualification. If cell bodies in the A laminae tend to be larger in the rostrocaudal dimension than are those in MIN, then

the conclusion may not be valid since the measurements were made from coronal sections. However, inspection of limited lateral geniculate material cut in the sagittal or horizontal plane indicates no obvious difference in the rostrocaudal dimension of these cell groups. Thus we tentatively conclude that MIN cells indeed tend to be larger in volume than cells in laminae A and A1.

This conclusion might be expected since Y-cells are thought to be larger than X-cells (for retina, see Boycott and Wässle, '74; Fukuda and Stone, '75; Cleland et al., '75; for the lateral geniculate nucleus, see LeVay and Ferster, '77), and thus a pure Y-cell population should be larger than one comprised of X- and Y-cells. However, the fact that many MIN relay cells are as small as the smallest relay cells in the A laminae (see also Lin et al., '77) suggests two possibilities. (1) Some MIN Y-cells might be smaller than their A laminae counterparts. It may be, for instance, that all A laminae Y-cells project both to areas 17 and 18 by virtue of a branching axon, and thus have larger soma to maintain multiple projections; whereas many MIN Y-cells project to only one cortical area. (2) On the other hand, it may be that considerable overlap exists in sizes between geniculate X- and Y-cells, and that the MIN sizes also reflect sizes for Y-cells in the A laminae. The data of LeVay and Ferster ('77) seem to support the second alternative; namely, that size differences between X- and Y-cells are much less clear in the lateral geniculate nucleus than they are in retina, that considerable overlap can occur between geniculate X- and Y-cell sizes, and therefore that MIN sizes seen here may reflect sizes of A laminae Y-cells. In support of this, Lin and Sherman ('78) have found that area 18 injections of horseradish peroxidase, which in laminae A and A1 apparently retrogradely label only geniculate Y-cells (Stone and Dreher, '73), produce a distribution of labelled cell sizes in the A laminae indistinguishable from the distribution of labelled cell sizes in MIN after extensive visual cortex injections of horseradish peroxidase.

Conclusions

It is clear that MIN Y-cells and Y-cells in laminae A and A1 of the geniculate share most or all fundamental features. If, as we have suggested, these cell groups should be considered subpopulations of a more general group of geniculate Y-cells, this raises interesting questions about the lateral geniculate nucleus and its evolution.

Unfortunately, too little is known about phylogenetic comparisons of X- and Y-cells to gain a perspective for the organization of the cat dorsal lateral geniculate nucleus. However, it has been reported that in the monkey's lateral geniculate nucleus there is a clear anatomical segregation between X-cells in the parvocellular laminae and Y-cells in the magnocellular laminae (Sherman et al., '76; Dreher et al., '76). The cat's MIN in some ways may be analogous to the monkey's magnocellular geniculate laminae since both represent a pure Y-cell population. Whether a true homology exists (does MIN represent an evolutionary stage in the anatomical segregation of X- and Y-cells that is more complete in the primate?) of course, cannot yet be answered.

ACKNOWLEDGMENTS

We thank S. Gibson and C. Hubbard for their expert technical assistance, and H. Sullivan for typing of the manuscript.

This research was supported by PHS Grant EY 01565. Further support from the PHS included Research Career Development Award EY 00020 to S. M. S. and Postdoctoral Fellowship EY 05077 to K. E. K.

LITERATURE CITED

Bishop, P. O., W. Kozak and G. J. Vakkur 1962 Some quantitative aspects of the cat's eye: Axis and plane of reference, visual field co-ordinates and optics. J. Physiol. (London), *163:* 466-502.

Boycott, B. B., and H. Wässle 1974 The morphological types of ganglion cells of the domestic cat's retina. J. Physiol. (London), *240:* 397-419.

Cleland, B. G., M. W. Dubin and W. R. Levick 1971 Sustained and transient neurones in the cat's retina and lateral geniculate nucleus. J. Physiol., *217:* 473-496.

Cleland, B. G., and W. R. Levick 1974 Brisk and sluggish concentrically organized ganglion cells in the cat's retina. J. Physiol., *240:* 421-456.

Cleland, B. G., W. R. Levick and H. Wässle 1975 Physiological identification of a morphological class of cat retinal ganglion cells. J. Physiol., *248:* 151-171.

Cowan, W. M., D. I. Gottlieb, A. E. Hendrickson, J. L. Price and T. A. Woolsey 1972 The autoradiographic demonstration of axonal connections in the central nervous system. Brain Res., *37:* 21-51.

Dreher, B., Y. Fukada and R. W. Rodieck 1976 Identification and anatomical segregation of cells with X-like and Y-like properties in the lateral geniculate nucleus of old-world primates. J. Physiol., *258:* 433-452.

Dreher, B., and A. J. Sefton 1975 Receptive field properties of cells in cat's medial interlaminar nucleus (MIN). Proc. Australian Physiol. Pharm. Soc., *6:* 209.

Enroth-Cugell, C., and J. G. Robson 1966 The contrast sensitivity of retinal ganglion cells of the cat. J. Physiol., *187:* 517-522.

Fernald, R., and R. Chase 1971 An improved method for

plotting retinal marks and focusing the eyes. Vision Res., *11:* 95-96.

Fukuda, Y., and J. Stone 1975 Direct identification of the cell bodies of Y-, X-, and W-cells in the cat's retina. Vision Res., *15:* 1034-1036.

Gilbert, C. D., and J. P. Kelly 1975 The projections of cells in different layers of the cat's visual cortex. J. Comp. Neur., *163:* 81-106.

Guillery, R. W. 1970 The laminar distribution of retinal fibers in the dorsal lateral geniculate nucleus of the cat: A new interpretation. J. Comp. Neur., *138:* 339-368.

Hayhow, W. R. 1958 The cytoarchitecture of the lateral geniculate body in the cat in relation to the distribution of crossed and uncrossed optic fibers. J. Comp. Neur., *110:* 1-64.

Hoffmann, K.-P., and J. Stone 1971 Conduction velocity of afferents to cat visual cortex: A correlation with cortical receptive field properties. Brain Res., *32:* 460-466.

Hoffmann, K.-P., J. Stone and S. M. Sherman 1972 Relay of receptive field properties in the dorsal lateral geniculate nucleus of the cat. J. Neurophysiol., *35:* 518-531.

Holländer, J., and H. Vanegas 1977 The projection from the lateral geniculate nucleus onto the visual cortex in the cat. A quantitative study with horseradish peroxidase. J. Comp. Neur., *173:* 519-536.

Hubel, D. H., and T. N. Wiesel 1965 Receptive fields and functional architecture of monkey striate cortex. J. Physiol. (London), *195:* 215-243.

Kinston, W. J., M. A. Vadas and P. O. Bishop 1969 Multiple projection of the visual field to the medial portion of the dorsal lateral geniculate nucleus and the adjacent nuclei of the thalamus of the cat. J. Comp. Neur., *136:* 295-315.

Kratz, K. E., S. V. Webb and S. M. Sherman 1978a Electrophysiological classification of X- and Y-cells in the cat's lateral geniculate nucleus. Vision Res., in press.

——— 1978b Effects of early monocular lid-suture upon neurons in the cat's medial interlaminar nucleus. J. Comp. Neur., *181:* 615-626.

Laties, A. M., and J. M. Sprague 1966 The projection of optic fibers to the visual centers in the cat. J. Comp. Neur., *127:* 35-70.

LeVay, S., and D. Ferster 1977 Relay cell classes in the lateral geniculate nucleus of the cat and the effects of visual deprivation. J. Comp. Neur., *172:* 563-584.

Lin, C. S., K. E. Kratz and S. M. Sherman 1977 Percentage of relay cells in the cat's lateral geniculate nucleus. Brain Res., *131:* 167-173.

Lin, C. S., and S. M. Sherman 1978 Effects of early monocular eyelid suture upon development of relay cell classes in the cat's lateral geniculate nucleus. J. Comp. Neur., in press.

Maciewicz, R. J. 1974 Afferents to the lateral suprasylvian gyrus of the cat traced with horseradish peroxidase. Brain Res., *84:* 308-312.

——— 1975 Thalamic afferents to areas 17, 18, and 19 of cat cortex traced with horseradish peroxidase. Brain Res., *84:* 308-312.

Mason, R. 1975 Cell properties in the medial interlaminar nucleus of the cat's lateral geniculate complex in relation to the transient/sustained classification. Exp. Brain Res., *22:* 327-329.

Palmer, L. A., A. C. Rosenquist and R. Tusa 1975 Visual receptive fields in lamLGNd, MIN, and PN of the cat. Neuroscience Abstr., *1:* 54.

Rosenquist, A. C., S. B. Edwards and L. A. Palmer 1974 An autoradiographic study of the projections of the dorsal lateral geniculate nucleus and posterior nucleus in the cat. Brain Res., *80:* 71-93.

Rowe, M. H., and J. Stone 1977 Naming of neurones. Brain, Behav. and Evol., *14:* 185-216.

Sanderson, K. J. 1971 The projection of the visual field to the lateral geniculate and medial interlaminar nuclei in the cat. J. Comp. Neur., *143:* 101-118.

——— 1974 Lamination of the dorsal lateral geniculate nucleus in carnivores of the weasel *(Mustelidae),* raccoon *(Procyonidae)* and fox *(Canidae)* families. J. Comp. Neur., *153:* 239-266.

Sanderson, K. J., P. O. Bishop and I. Darian-Smith 1971 The properties of the binocular receptive fields of lateral geniculate neurons. Exp. Brain Res., *13:* 178-207.

Shapley, R., and S. Hochstein 1975 Visual spatial summation in two classes of geniculate cells. Nature, *256:* 411-413.

Sherman, S. M., T. T. Norton and V. A. Casagrande 1975 X- and Y-cells in the dorsal lateral geniculate nucleus of the tree shrew *(Tupaia glis).* Brain Res., *93:* 152-157.

Sherman, S. M., and J. R. Wilson 1975 Behavioral and morphological evidence for binocular competition in the postnatal development of the dog's visual system. J. Comp. Neur., *161:* 183-196.

Sherman, S. M., J. R. Wilson, J. H. Kaas and S. V. Webb 1976 X- and Y-cells in the dorsal lateral geniculate nucleus of the owl monkey *(Aotes trivergatus).* Science, *192:* 475-477.

Stone, J. 1972 Morphology and physiology of the geniculocortical synapse in the cat: The question of parallel input to striate cortex. Invest. Ophthalmol., *11:* 338-346.

Stone, J., and B. Dreher 1973 Projection of X- and Y-cells of the cat's lateral geniculate nucleus to areas 17 and 18 of visual cortex. J. Neurophysiol., *36:* 551-567.

Wilson, P. D., and J. Stone 1975 Evidence of W-cell input to the cat's visual cortex via the C-laminae of the lateral geniculate nucleus. Brain Res., *92:* 472-478.